

# **Solving Partial differential equations using the Finite difference method**

By khalil pierre

*This aims of this investigation were to use finite difference methods to find numerical solutions of Laplace's equation and the Heat equation.*

## **1. Background**

Partial differential equations (PDEs) are vital in describing the behaviour of a multitude of different physical systems. The solutions to PDEs can be approximated using the finite difference method<sup>[1]-[4]</sup>. The finite difference method essentially converts a continuous sample space into a discrete sample space<sup>[1][3]</sup>. The finite difference method approximates the solution to PDEs by writing the derivatives of a differential equation as either a forward central or backwards finite difference

$$\frac{df}{dx} \approx \frac{f(x_{i+1}) - f(x_i)}{h}, \quad (1)$$

$$\frac{df}{dx} \approx \frac{f(x_i) - f(x_{i-1}))}{h}, \quad (2)$$

$$\frac{df}{dx} \approx \frac{f(x_{i+1}) - 2f(x_i) + f(x_{i-1}))}{2h}, \quad (3)$$

where  $h$  is the spacing between point in the discrete position space, equation 1 is the forward finite difference, equation 2 in the backwards finite difference and equation 3 in the central finite difference<sup>[1]</sup>. Equation 1 and 2 are derived by taking the Taylor series of a function about the point  $x_i$ , solving for  $df/dx$  and ignoring all higher order terms<sup>[1][3]</sup>. Equation 3 is derived by taking the difference of equation 1 and 2<sup>[1][3]</sup>. By truncating an infinite Taylor series both equation 1 and 2 will have an error of order  $h$  whilst equation 3 will be more accurate and have an error of order  $h^2$ .

This exercise looked at solving Laplace's equation

$$\nabla^2 V = 0, \quad (4)$$

( $V$  is the electrostatic potential) and the heat equation

$$\alpha \nabla^2 \varphi = \frac{\partial \varphi}{\partial t}, \quad (5)$$

where  $\varphi$  is the temperature,  $t$  is time and  $\alpha$  is the diffusion coefficient. Both equation 4 and 5 contain second order partial derivatives. Second order derivatives can be approximated using the second order central finite difference equation<sup>[1][3]</sup>

$$\frac{d^2 f}{dx^2} \approx \frac{f(x_{i+1}) - 2f(x_i) + f(x_{i-1}))}{h^2}. \quad (6)$$

## **2. Task 1 Laplace's equation**

The first task was to solve the 2D Laplace equation. To do this the position space had to be discretized into a 2D mesh grid where each node on the mesh grid had an  $x$  and  $y$  coordinate. Using equation 4 and equation 6 the potential at any point on the mesh grid can be writing as

$$V(x_i, y_i) = \frac{1}{4} (V(x_{i+1}, y_j) + V(x_{i-1}, y_j) + V(x_i, y_{j+1}) + V(x_i, y_{j-1})). \quad (7)$$

To find the potential for a system of interest appropriate boundary conditions need to be applied. An initial solution is then guessed and applied to every point on the grid. By using equation 7 and iterating over every point on the grid the initial guess will relax to a final solution. To stop the program from iterating over the grid indefinitely a convergence conditions must be chosen. The convergence condition that was used in this assignment was

$$\frac{1}{N} \sum_{i,j} V_{new}(x_i, y_j) - V_{old}(x_i, y_j) = Tol, \quad (8)$$

Where tol is a chooses tolerance. When the convergence condition is meet the program will stop running. This convergence condition was chosen to avoid any local convergence in the grid from causing the program to stop running.

There are two different methods for iterating over the mesh grid the Jacobi and the Gauss Seidel method. The Jacobi method updates each point on the grid from the values of previous grid whilst the Gauss Seidel method updates each point on the grid continually meaning that the value of each node is calculated using a mix of new and old values. The Gauss seidel method should be done in half the number of iterations as the Jacobi <sup>[2]</sup>. To test the accuracy of each method and to see which method to use in the proceeding investigation the potential of a grounded square box was evaluated. The boundary nodes of the grid were set to zero and all the non-boundary nodes were set to some random number between 1 and ten. The boundary nodes would be ignored during each iteration to preserve the boundary conditions. The potential field inside the box should be zero everywhere. Below are the results:

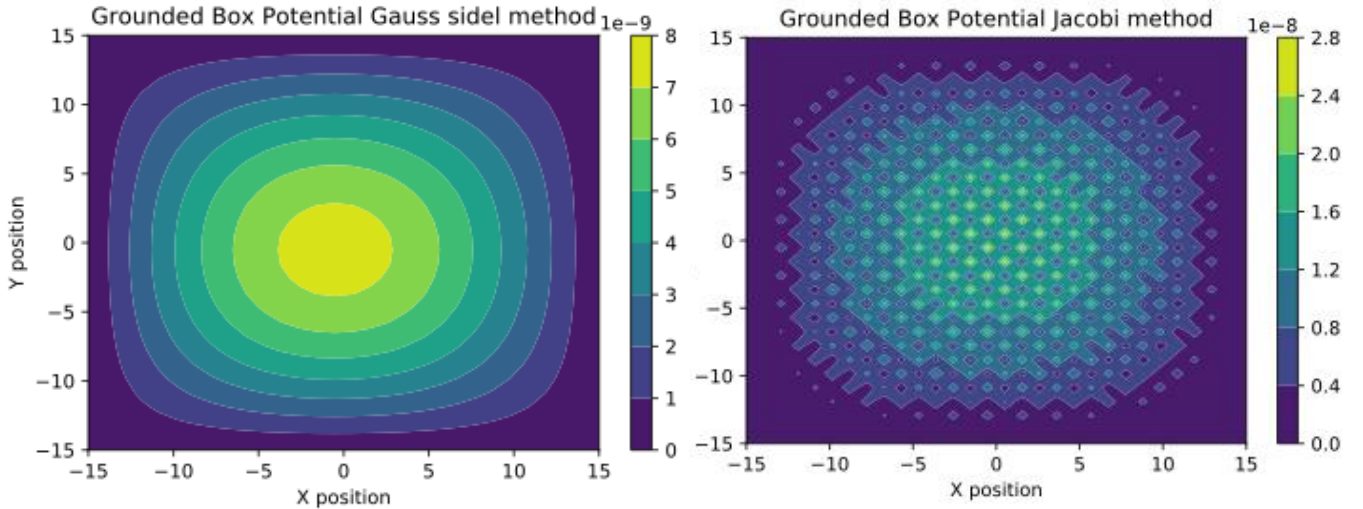


Figure 1 Potential field for a Grounded square box produced using the Gauss Seidel method (Left) and Jacobi method (Right) for a 30X30 grid and a tolerance of  $1e-9$ .

As you can see both methods approach the analytical solution and have potential field values that are comparable to the tolerance. Appendix figure 1 shows that the Gauss Sidle method takes half as many iterations as the Jacobi method regardless of the grids size. Appendix figure 2 also shows that the difference in accuracy between the Gauss Seidel and Jacobi methods grows exponentially as grid size increases. It was because of the difference in iteration times and accuracy that the Gauss Seidel method was chosen for the next part of the investigation.

The Gauss Seidel method was used to find the potential and electric field of a parallel plate capacitor. To do this the values of two sets of nodes that represent each capacitor were set to have a potential of  $\pm 1000$ . Both sets of capacitor nodes were ignored during each iteration. As the grid has finite dimensions the boundary nodes couldn't be evaluated using equation 7. The potential of a parallel plate capacitor should go to zero at infinity and so the boundary nodes were chosen to be zero. This is an accurate approximation when the grid dimensions are much greater than the capacitor dimensions.

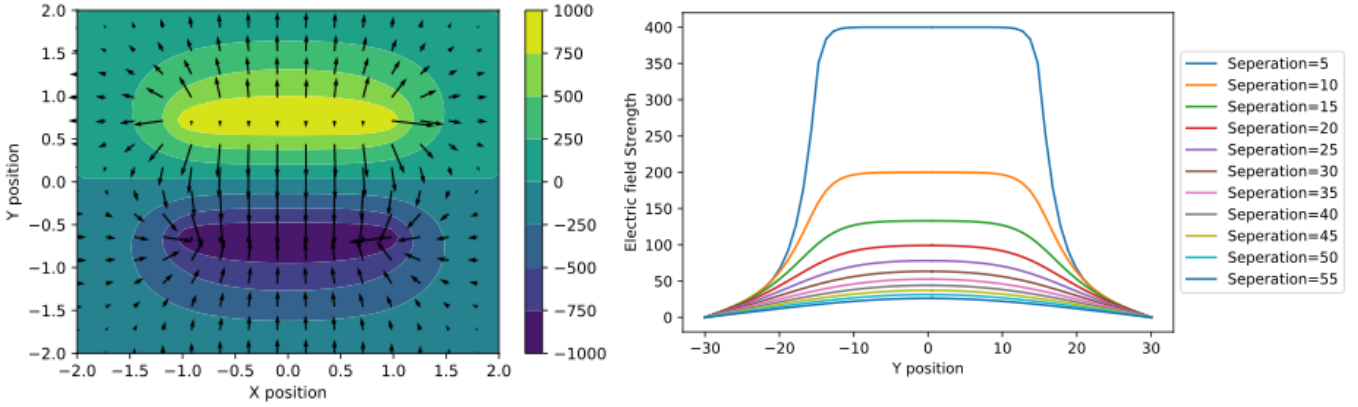


Figure 2 Left: Potential and electric field of parallel plate capacitors where the contour plot shows the potential field strength of the capacitor at each position and the vector lines show the strength and direction of the electric field at each position. Right: Horizontal slice of the y component of the electric field at the centre of the capacitor for different capacitor separations. The width of the capacitor is 20 nodes.

The left plot of figure 2 shows the problem with setting the Boundary nodes to 0 there is a resultant electric field outside of the capacitors due to the potential difference between the capacitor plates and the grid walls. A potential solution to this problem may be to update equation 4 at the boundaries to average over the values of the 3 adjacent nodes (2 at the corners). The right-hand side plot in figure 3 shows that as the width of the capacitor increases the electric field distribution better approximates the infinite plate solution i.e. a top hat function where the E field is contained entirely within the capacitor plates. However, because the electric field induced by the grounded walls we cannot assess whether the E field goes to zero outside of the plates. Appendix figure 3 also shows that the electric field inside the capacitor follows  $E=V/D$  better at smaller grid separations.

### 3. Task 2 Diffusion

The second task of this exercise was to find the temperature at some time  $t$  along a 1D metal rod. The metal is initially at room temperature and then the tip of the rod is placed into a furnace at 1000 degrees. To solve this problem the heat equation is expanded using equation 6 for the spatial derivative and equation 2 for the temporal derivative which gives <sup>[1]</sup>:

$$\frac{\varphi'_i - \varphi_i}{\Delta t} = \alpha \frac{\varphi'_{i-1} + \varphi'_{i+1} - 2\varphi'_i}{h^2} \quad (9)$$

$\Delta t$  is the time step between iterations,  $\varphi_i$  is the temperature of the rod at some point  $x_i$  and time  $t$  and  $\varphi'_i$  is the temperature at the point  $x_i$  at the time  $t+\Delta t$ . Solving equation 9 for  $\varphi_i$  results in:

$$\varphi_i = (1 + 2\gamma)\varphi'_i - \gamma\varphi'_{i+1} - \gamma\varphi'_{i-1} \quad (10)$$

Where  $\gamma = \frac{\alpha}{h^2} \Delta t$ . If the rod is divided into 4 grid points and equation 10 is applied to each grid point, then the temperature of each point in our grid is set up by a series of linear equations. However careful consideration is needed when we consider the endpoints of our rod as equation 10 would require points that are out of bounds (ghost nodes). The values of these ghost nodes depend

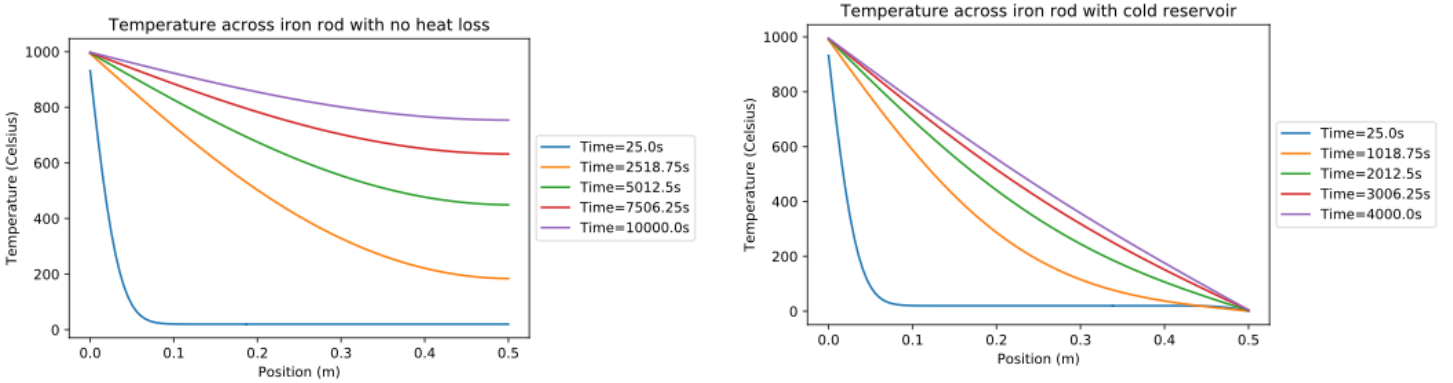
on the boundary conditions. If the temperature at one end of the rod is held constant, then the value of the ghost node can be found by saying that the average of the end node and ghost node is equal to the boundary temperature which gives<sup>[4]</sup>

$$\Rightarrow \phi_{ghost} = 2T_0 - \phi_{boundary} \quad (11)$$

where  $T_0$  is the boundary temperature. If there is no heat loss from the end of the rod, then the gradient of  $\phi$  goes to zero across the rod. Using equation 1 as an approximation of the gradient gives  $\phi_{ghost} = \phi_{ghost}$ . Putting this all together results in the tridiagonal matrix shown below

$$\begin{pmatrix} 1+3\gamma & -\gamma & 0 & 0 \\ -\gamma & 1+2\gamma & -\gamma & 0 \\ 0 & -\gamma & 1+2\gamma & -\gamma \\ 0 & 0 & -\gamma & X \end{pmatrix} \cdot \begin{pmatrix} \phi'_{i-2} \\ \phi'_{i-1} \\ \phi'_i \\ \phi'_{i+1} \end{pmatrix} = \begin{pmatrix} \phi_{i-2} + 2\gamma T_1 \\ \phi_{i-1} \\ \phi_i \\ \phi_{i+1} \end{pmatrix} \quad (12)$$

Where X and Z depends on what boundary condition you are using and  $T_1$  is the temperature of the furnace (1000°C). X is equal to  $1+3\gamma$  when the second end of the rod is kept at 0°C and X is  $1+\gamma$  when there is no heat loss from the rod. The temperature distribution across the rod for both case's is



shown below.

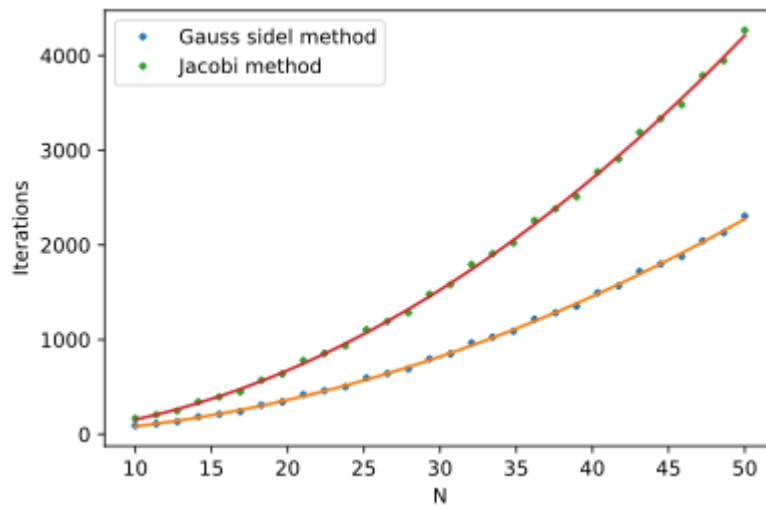
Figure 3 Temperature across the iron rod for different total times. Left: The left-hand side of the rod is in contact with a furnace at 1000 degrees and no heat loss is allowed. Right: The left-hand side of the rod is in contact with a furnace at 1000 degrees and the right-hand side is in contact with an ice bath at zero degrees.

As time goes on the left plot shows that the temperature of the rod everywhere continues to rise. This is what is expected as no heat loss is allowed, and the system will eventually reach equilibrium where all points along the rod are at 1000 degrees. The right-hand plot also shows what is expected at equilibrium is a linear temperature gradient across the rod where the left hand side is at 1000 degrees and the right hand side is at 0 degrees.

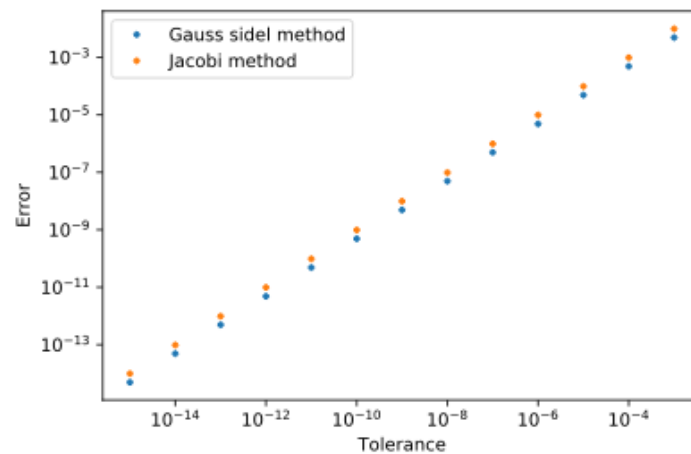
## References

1. brooke, J. (2019). *Computational physics lecture 1*. University of bristol.
2. H, W., Teukoisky, S. A., Vetterling, W. T., & flannery, B. P. (1986). *Numerical recipes the art of Scientific computing third edition*. Cambridge university press.
3. Nagel, J. R. (2011). *Solving the Generalized Poisson Equation Using the*. Salt Lake City: University of Utah.
4. V. Vuorinen. (2017). *Finite Difference Methods in Heat*. Aalto University School of Engineering.

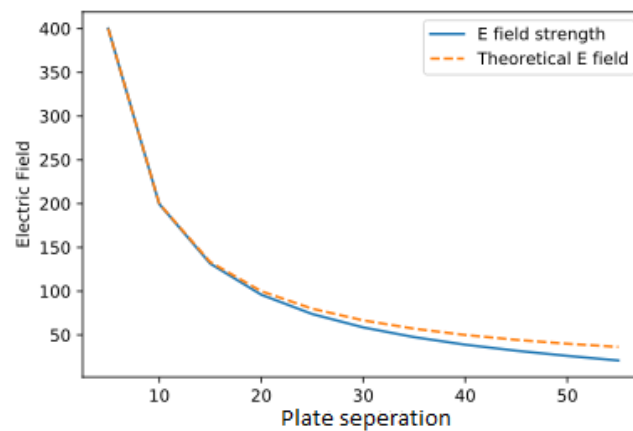
## Appendix:



Appendix Figure 1: Plot of number of iterations until convergence condition is met against grid size for simple square box potential. Both the Jacobi and Gauss sidle are fitted with quadratic plot.



Appendix Figure 2: Plot of numerical error against tolerance for simple square box potential. Both the x and y axis are log scaled. The numerical error was taken as the largest node value as the potential should be zero everywhere.



Appendix Figure 2: Electric field strength within the capacitor plotted against plate separation.